

New alloying concepts for increased corrosion resistance of welded linepipe steels in CO₂ containing aqueous media

M. Tröger, C. Bosch, Salzgitter Mannesmann Forschung, Duisburg, Germany

H. Meuser, Salzgitter Mannesmann Grobblech, Mühlheim, Germany

F. M. Knoop, Salzgitter Mannesmann Großrohr, Salzgitter, Germany

H. Brauer, Salzgitter Mannesmann Linepipe, Hamm, Germany

J. Schröder, Europipe GmbH, Mülheim, Germany

ABSTRACT

For investigation of the corrosion behaviour of low alloyed carbon steels for applications in CO₂ containing aqueous media new alloying concepts with linepipe steel chemical compositions were defined and tested by means of laboratory melts. Two reference steels and four alloy variations were produced to develop alternative steels to the classical 0.5 % Cr steels with increased corrosion resistance in wet CO₂ taking into account the weldability of the steels. For identification of suitable alloys chromium contents between 0.1 and 0.5 % were tested with systematic variations of the alloying elements Cu, Mo, Ni and V. Laboratory tests were performed to determine the CO₂ corrosion resistance in 0.1 % sodium chloride solution on flat specimens in the rotating cage under 1 bar (0.1 MPa) CO₂ at 40 and 80 °C and 1 m/s average flow velocity. The susceptibility of the heat affected zone (HAZ) of the steels to localized corrosion was evaluated using submerged-arc-welded (SAW) samples prepared in the lab. With regard to general corrosion an improvement of the corrosion resistance up to 30 % was obtained for additions of both Cu and V and a combination of Cr, Ni and V. At high temperature conditions a higher alloyed steel containing Cr, Mo, Ni, Cu and V is the best alternative showing good resistance to localized corrosion of the base material and the HAZ.

INTRODUCTION

In transmission oil and gas pipelines and well-head applications the majority of corrosion problems are associated with the presence of CO₂ and/or H₂S. Carbon dioxide corrosion is affected by many parameters and can cause significant localized and uniform corrosion. A particular issue is that for localized attack very high corrosion rates may occur leading to premature failure. Different strategies are pursued to ensure a sufficient corrosion resistance of oil and gas pipelines in CO₂ containing aqueous media. For oil and gas wells highly alloyed 13Cr steels or duplex stainless steels are often used to avoid premature failure especially in down-hole applications. Due to economic and weldability issues highly alloyed steels are not used for transmission pipelines. For this application carbon steels and low-alloy steels in combination with corrosion inhibitors and/or coating systems are generally the first choice.

The durability of oil and gas pipelines under sweet corrosion conditions mainly depends on whether protective or non-protective corrosion product scales are formed. This is affected by different parameters such as temperature, flow velocity, CO₂ partial pressure or medium composition [1-3]. Lab as well as field experiments have shown that beside the influence of medium-related and interphase-related parameters, material

properties such as chemical composition, heat treatment and microstructure can play a significant role for uniform and localized carbon dioxide corrosion.

The influence of alloying elements on the corrosion resistance of linepipe steels in CO₂ containing aqueous solutions was subject of various studies the last 10-15 years [4-17]. Most of the research related to the effect of chemistry is focused on the influence of chromium [5, 7-13]. Due to the demand to decrease CAPEX and OPEX in the oil and gas industry there is a growing interest for the development of low-alloy steels with increased chromium contents of up to 3 %. By enrichment in the corrosion product scale chromium can promote the formation of more protective passive films resulting in a considerable decrease of the corrosion rate [2, 5, 7-14]. Medium chromium alloyed steels between a conventional L80 API 5CT and a 13Cr steel provide an improved corrosion resistance and at the same time an acceptable increase in costs compared to carbon steels. Even chromium additions of 0.5 % reveal improved corrosion resistance by a factor of two compared to API X65 [4]. However, contradictory results are reported regarding the effective amount of chromium owing to the fact that material parameters such as microstructure or heat treatment as well as testing conditions can have an additional influence [3, 6, 10, 15].

Numerous studies focused not only on the effect of chromium but investigated the influence of minor additions of other elements, e.g. Cu, Ni, Mo, V or Ti in order to increase the CO₂ corrosion resistance [6, 10-16]. The approach followed is to avoid Cr carbides to have sufficient Cr available in solid solution for enrichment in the passive film. This can be realized by a reduction of the carbon content [5, 17] or by an addition of microalloying elements such as V, Ti or Nb which form more stable carbides [10, 11, 16].

This paper reports on laboratory tests on six different linepipe steel compositions with 0.1 to 0.5 % Cr to determine the CO₂ corrosion resistance in 0.1 % sodium chloride solution under moderate flow conditions. The study was focused on the influence of the alloying elements Cu, Mo, Ni and V in order to develop alternatives to 0.5 % Cr steels with improved CO₂ corrosion resistance taking into account the weldability. The influence of different microstructure of the base metal and weld area on general as well as localized corrosion of the materials was examined.

EXPERIMENTAL PROCEDURE

Material

Six laboratory heats of 100 kg each were produced with different chemical compositions suitable for linepipe steels. Plates were rolled to a thickness of 20 mm and submerged arc welded by use of chromium free wires. The chemical composition of the alloy variations are shown in Table 1. The concentration of Cr, V, Cu, Ni and Mo were varied based on a standard linepipe chemical composition in order to investigate the influence of the elements. Two reference steels were defined, either with 0.5 % Cr or without additional alloying elements. Two heats contained Cu and different amounts of V. The chromium content was increased to a medium concentration of 0.3 % for the last two heats. The effect of Ni was investigated by one of these steels and the effect of Mo, Ni and Cu by the other. V content was kept constant.

After thermomechanical rolling strength properties of grade X70 were reached for both reference materials and grade X80 for the higher alloyed materials D, E and F. All materials show a predominantly ferritic microstructure with small amounts of pearlite. Material F contains about 15 % bainitic fractions (Figure 1).

A picture of the submerged arc weld of material E is given in Figure 2 together with the corresponding microstructure of the inner weld and of the transition area of coarse grained zone to fine grained zone (HAZ).

Two of the heats, material B and E, were used to simulate the high-frequency induction (HFI) method representing the production process of longitudinal HFI welded linepipe steels. For this process plate material with a thickness of 6 mm was used. After welding the HFI specimens were annealed.

Table 1: Chemical composition of the laboratory heats (mass-%)

reference	material	C	P	S	Cr	Mo	Ni	Cu	V	Others
A	reference 0.5%Cr	0.06	< 0.02	< 0.002	0.5					Si, Mn, Nb, Ti
B	reference unalloyed	0.06	< 0.02	< 0.002	0.1					
C	Cu4V	0.06	< 0.02	< 0.002	0.1			0.25	0.04	
D	Cu8V	0.06	< 0.02	< 0.002	0.1			0.25	0.08	
E	CrNiV	0.06	< 0.02	< 0.002	0.3		0.25		0.08	
F	CrMoNiCuV	0.06	< 0.02	< 0.002	0.3	0.3	0.25	0.25	0.08	

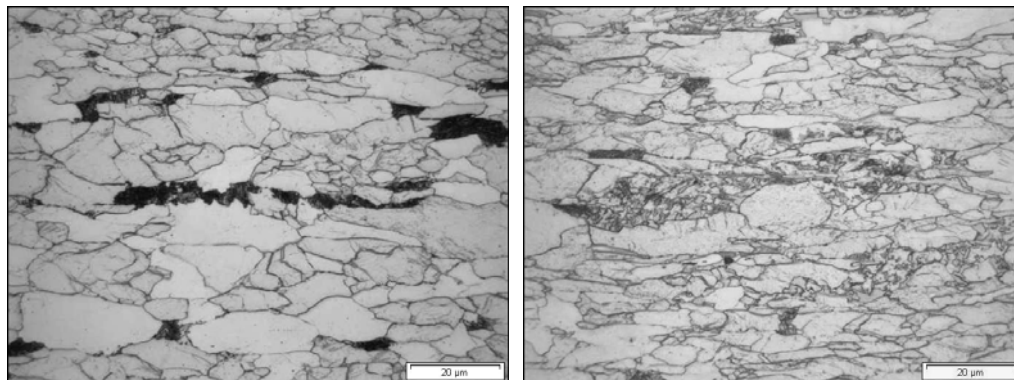


Figure 1: Microstructure of material B (left) and material F (right)

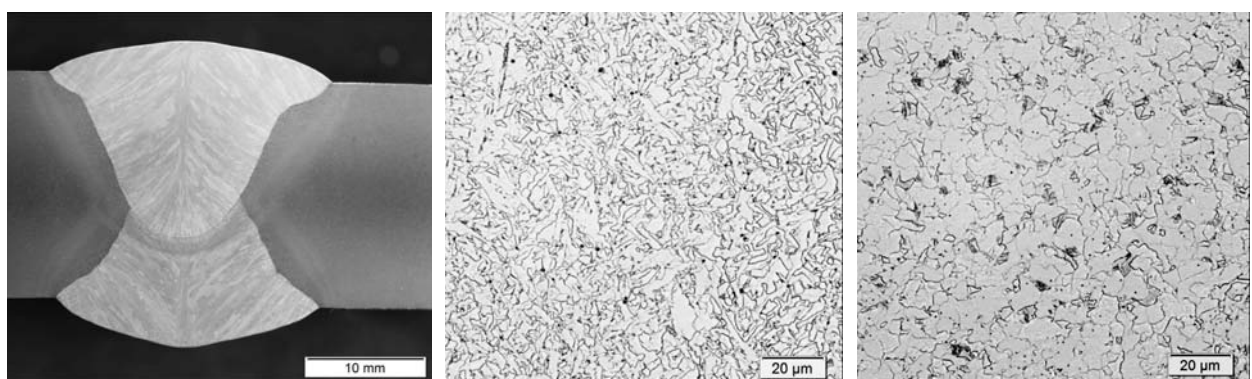


Figure 2: Submerged arc weld of material E (left) and microstructure of the inner weld (middle) and heat affected zone (right)

Rotating cage experiments

For the rotating cage experiments flat specimens of the dimension 50 x 10 x 5 mm were used. For the base metal specimens were taken longitudinal to the rolling direction and in case of the weld transverse to the weld.

The experiments were performed in 0.1 % sodium chloride solution at 1 bar (0.1 MPa) CO₂ at 40 and 80 °C with a rotation of 167 Rpm. This rotation corresponds to an aver-

age velocity of 1 m/s at the outer surface of the flat coupons in the rotating cage. The test duration was 336 hours (14 days). The coupons were mounted between two discs machined from polytetrafluoroethylene and rotated in the solution with the desired rotation speed. A constant temperature was maintained by heating plates controlled by contacting thermometers.

Prior to testing the specimens were degreased, weighed and mounted in the test vessel. Four coupons were taken per material in one coupon holder and test vessel. The closed vessel was then purged with nitrogen for a minimum of 1 hour. The N₂ purged and pre-heated test solution was then filled in the vessel and after reaching the test temperature continuous CO₂ bubbling was started. The pH and Fe content of the test solution were measured in regular intervals. After the end of the experiment the specimens were pickled in inhibited hydrochloric acid and subjected to mass loss measurement in order to calculate the integral corrosion rate.

One set of corrosion samples was subject to SEM investigations for further investigation of the corrosion product scales. For this purpose weld samples of the experimental series at 80 °C were chosen. Cross sections were taken directly after the rotating cage experiment and embedded in epoxy resin.

RESULTS

Base material

The integral corrosion rates of the rotating cage experiments of the base metal determined by mass loss measurements are summarized in Figure 3. Samples of the base material were tested for all materials at 40 and 80 °C. The integral corrosion rates ranged between 0.76 and 2.0 mm/y dependent on alloy composition and test temperature. At 40 °C the average corrosion rates vary between 1.12 and 2.0 mm/y whereas materials D and E presented the best corrosion behavior. As expected, the unalloyed reference material showed a comparatively high corrosion rate of 1.76 mm/y while the corrosion rate of 2.0 mm/y obtained for the higher alloyed material F was rather unexpected.

In general, an increase of the test temperature to 80 °C resulted in a reduction of the corrosion rates with values between 0.76 and 1.6 mm/y. However, for the 0.5 % Cr steel an increase of the corrosion rate from 1.4 to 1.6 mm/y was observed. The best corrosion behavior under the condition of the test series at 80 °C was measured for the higher alloyed material F. Comparing the materials under both test conditions materials D and material E showed a good corrosion behavior at both test temperatures.

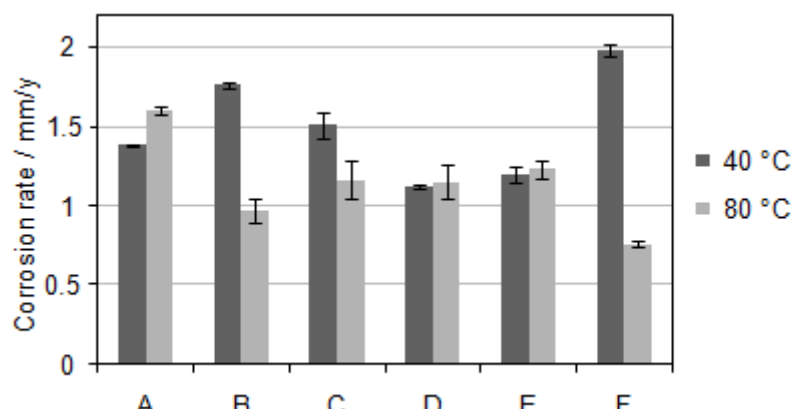


Figure 3: Corrosion rates of the base metals at 40 and 80 °C from mass loss measurements (rot. cage, 0.1 % NaCl, 1 bar (0.1 MPa) CO₂, 1 m/s)

Corrosion samples were examined visually after test end and pickling in inhibited hydrochloric acid. At 40 °C general corrosion was predominant as no protective corrosion product scales were able to form under these conditions. Specimens exposed at 80 °C revealed localized attack and flow induced corrosion for material B, C and D while the other materials showed no susceptibility to localized corrosion (Figure 4).

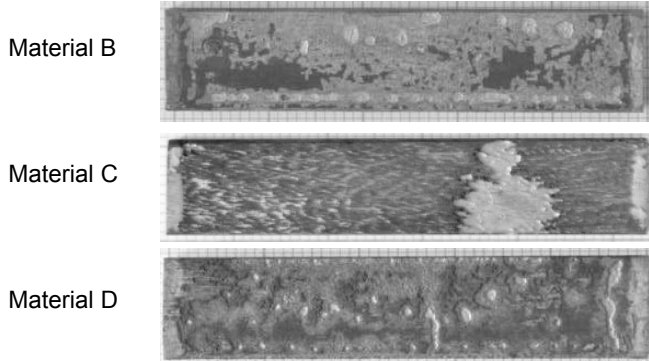


Figure 4: Specimen surface of rotating cage samples of the base metal tested at 80 °C after pickling in inhibited hydrochloric acid, magnification 1.3

The evolution of the iron content of the test solutions with test time is given in Figure 5 for both test series. After test start the iron content increases continuously until test end reaching values between 25 and 58 mg/l for a temperature of 40 °C and values between 6 and 24 mg/l at 80 °C. An increase of the test temperature which resulted in reduced corrosion rates also caused a decrease of the iron content. Furthermore iron contents measured for the test series at 80 °C indicate that reasonably constant values are reached after about one third of the test time.

The pH of the test solutions ranged between 5.0 and 6.4 at a temperature of 40 °C and between 5.2 and 5.6 in case of the test series at 80 °C.

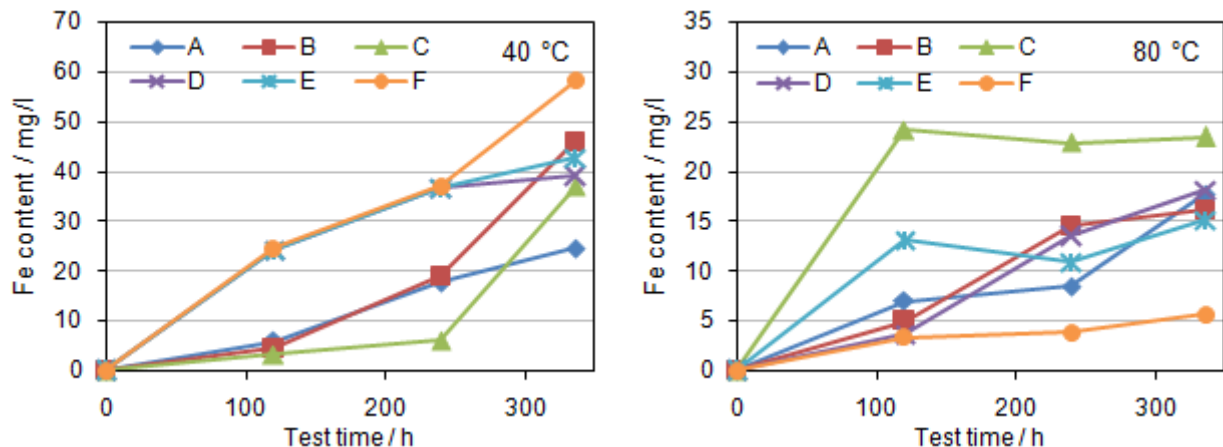


Figure 5: Evolution of the Fe-content at 40 °C (left) and 80 °C (right) with test time, base metal (rot. cage, 0.1 % NaCl, 1 bar (0.1 MPa) CO₂, 1 m/s)

Weld material

The results obtained for the rotating cage experiments of the weld specimens (SAW) are given in Figure 6 for both temperatures. At 40°C the average corrosion rates ranges between 1.2 and 2.1 mm/y and thus are comparable to the values obtained for the base

metals. Again materials D and E presented the best corrosion behavior while material F shows the highest susceptibility to corrosion under the tested conditions.

In the test series with a temperature of 80 °C corrosion rates between 0.7 and 1.9 mm/y were determined with the lowest corrosion rate for material C. An unexpected increase of the corrosion rate from 1.3 to 1.9 mm/y was measured for material D. Good corrosion behavior with corrosion rates in the range of 1 mm/y was observed for materials A, E and F. A comparison of the results at both test temperatures confirms the different corrosion behavior of the materials dependent on the test temperature.

Rotating cage experiments with HFI welded specimens resulted in a slightly better corrosion behavior in case of material E compared to the SAW specimens. In contrast to this, for the unalloyed reference material B a higher corrosion rate was determined.

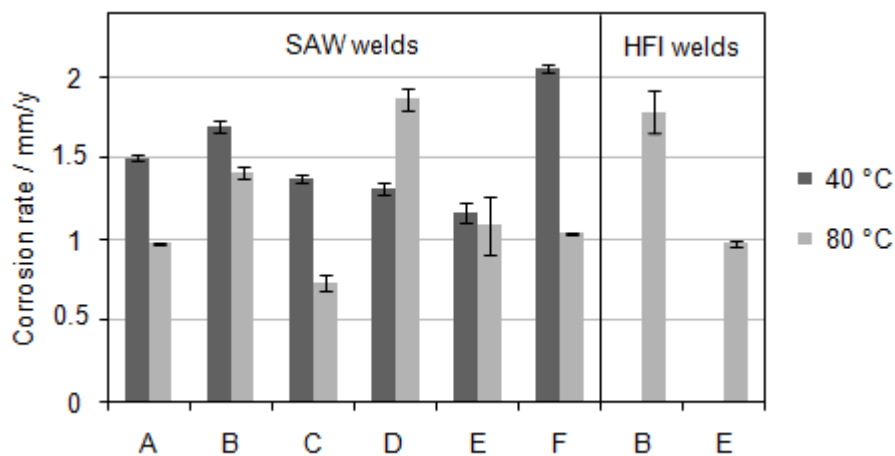


Figure 6: Corrosion rates of the weld samples (SAW and HFI) at 40 and 80 °C from mass loss measurements (rot. cage, 0.1 % NaCl, 1 bar (0.1 MPa) CO₂, 1 m/s)

Visual examination of the specimens after test end and pickling in inhibited hydrochloric acid revealed uniform corrosion with no indication of preferential corrosion or localized attack for all samples exposed at 40 °C. For the test series with a temperature of 80 °C the appearance of the rotating cage specimens containing a submerged arc weld is exemplified in Figure 7. Both reference materials as well as material D show preferential corrosion of the base material and the HAZ and in case of material B and D localized attack of the weld can be seen while the weld seam of material A does not show any localized corrosion. For the corrosion samples of material C localized attack could be observed in all areas independent of the weld. The appearance of the higher alloyed materials E and F revealed more uniform corrosion. However, indications for slight localized attack were observed in case of material E at the transition of the heat affected zone and the weld and in case of material F in the weld.

Pictures of the corrosion samples containing the HFI weld are given in Figure 8. Both materials show localized corrosion outside the weld area with higher localized attack for the unalloyed reference material.

The iron content of the test solutions containing the weld specimens is displayed in Figure 9 dependent on the test time. A continuous increase of the iron contents with test time up to a maximum of 51 mg/l could be observed for most of the materials at both test conditions. Some of the materials showed a maximum iron content after one or two thirds of the test time indicating that constant test conditions were reached.

The pH of the test solutions ranged between 4.5 and 5.3 at a temperature of 40 °C and between 4.8 and 5.5 in case of the test series at 80 °C.

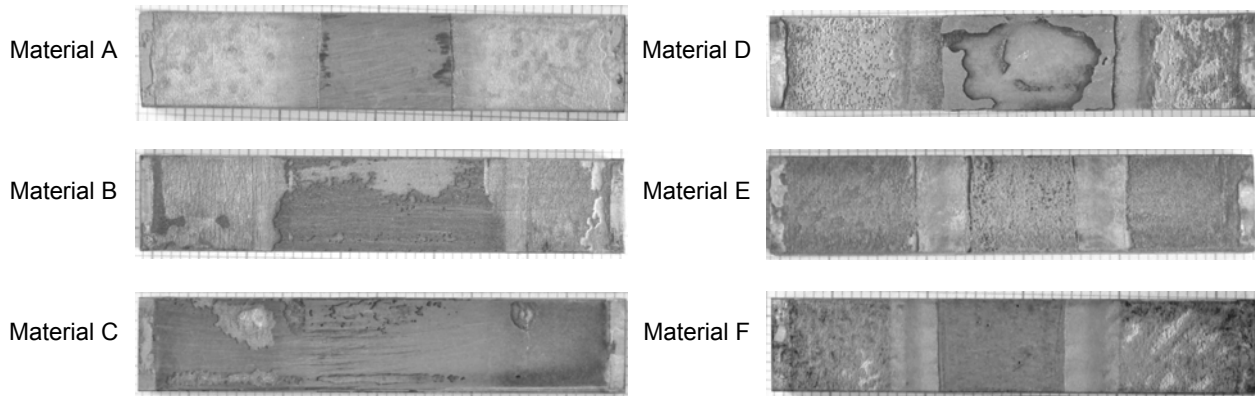


Figure 7: Specimen surface of rotating cage samples of the weld metal tested at 80 °C after pickling in inhibited hydrochloric acid, magnification 1.3

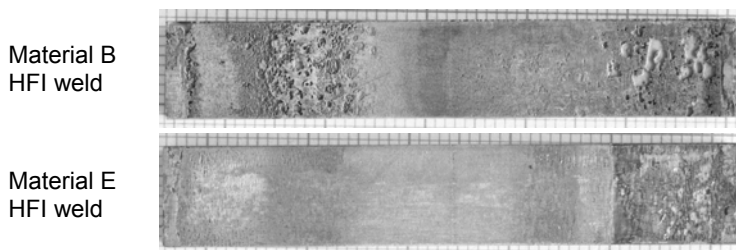


Figure 8: Specimen surface of rotating cage samples with the HFI weld tested at 80 °C after pickling in inhibited hydrochloric acid, magnification 1.5

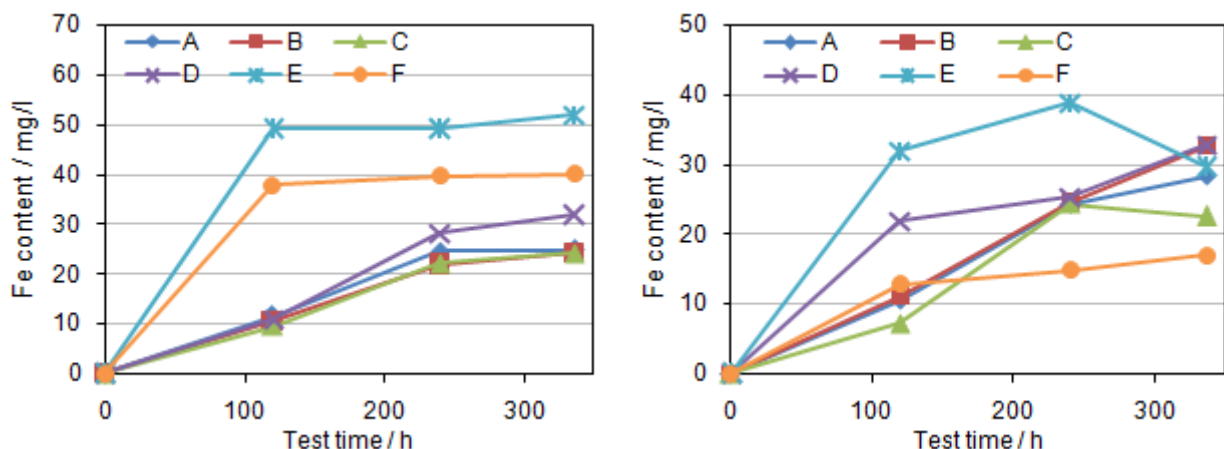


Figure 9: Evolution of the Fe-content at 40 °C (left) and 80 °C (right) with test time, weld specimens (rot. cage, 0.1 % NaCl, 1 bar (0.1 MPa) CO₂, 1 m/s)

In order to further examine the corrosion product layers and the preferential localized attack weld specimens which were tested at 80 °C were analyzed in the SEM. The investigation revealed corrosion product scales up to a thickness of about 110 µm with no significant difference between the materials. Samples show parts with different morphologies of the corrosion product scale. Porous networks presumably consisting of cementite and more densely packed phases of FeCO₃ were observed. SEM images of the surface layer of some of the materials are illustrated in Figure 10. In the transition zone of the heat affected zone and the weld seam of material A the cementite film on the surface seems to be sealed by a thin and compact FeCO₃ layer. Other surface

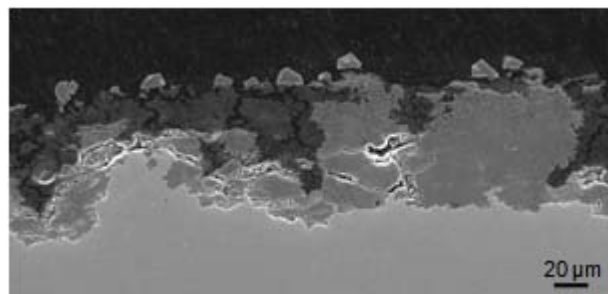
areas show a more inhomogeneous structure and mix of the corrosion products indicating the influence of the microstructure of the steel [3].

Samples were analyzed with regard to local metal loss in order evaluate the susceptibility of the steels and welds to localized attack. The results of these investigations are exemplified in Table 2 for four samples. The maximum difference of metal loss between the weld seam and the base metal was 68 µm determined for material B. This value is equivalent to a local difference of corrosion rate between weld and base metal of 1.77 mm/y. Local corrosion attack of the base material was observed for material B, C and D while for material E, preferential corrosion attack at the transition of base metal, heat affected zone and weld seam was found.

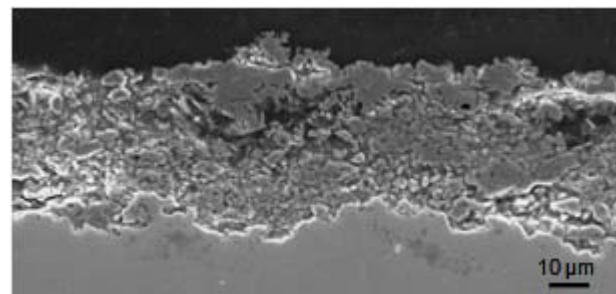
The qualitative composition of the corrosion products were analyzed by EDX to get an idea of the different phases observed. The presence of both cementite phases and iron carbonate phases were confirmed as well as the enrichment of alloying elements near the interface to the steel surface depending on the chemical composition of the materials.

Table 2: Local differences of metal loss between weld seam and base metal and corresponding local corrosion rates after rotating cage experiments at 80 °C

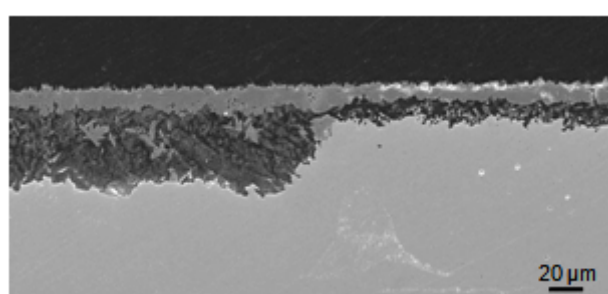
reference	material	Difference of metal loss / µm	Difference in corrosion rate / mm/y
A	reference 0,5%Cr	45	1.17
B	reference unalloyed	68	1.77
C	Cu4V	29	0.76
D	Cu8V	41	1.10



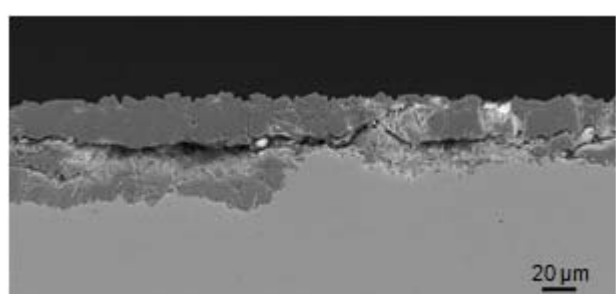
Material E - base material



Material F - base material



Material A - transition zone weld seam to base material



Material C - transition zone weld seam to base material

Figure 10: Corrosion product scales and localized corrosion of rotating cage samples tested at 80 °C after pickling in inhibited hydrochloric acid

DISCUSSION

Under the conditions where amorphous and less protective corrosion product scales are formed uniform corrosion dominates and was observed for all materials tested. The best performance was obtained for materials D and E alloyed with Cu and V and with Cr, Ni and V, respectively. Figure 11 illustrates the effect of the elements selected for systematic alloying of the heats on the average corrosion rates of the test series at 40 °C.

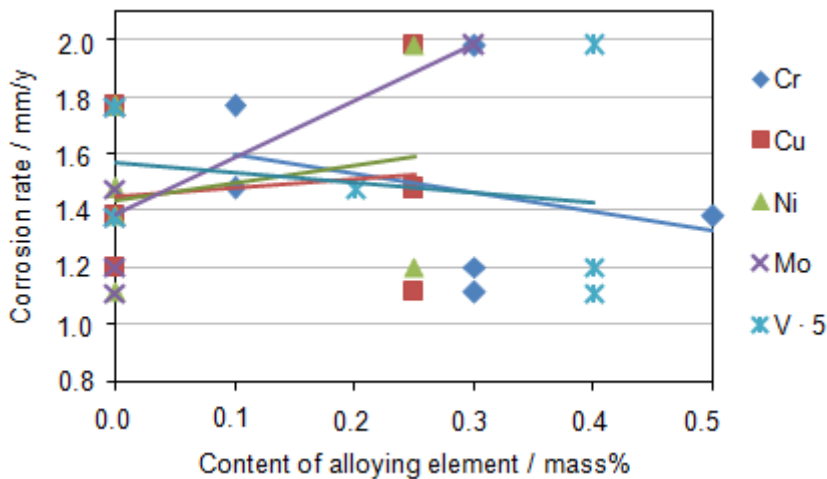


Figure 11: Relative effect of microalloying elements on the corrosion rate; vanadium content is multiplied by a factor of 5

The results show a positive effect only for Cr and V while for the other elements no significant effect or even a negative effect (Mo and Ni) can be seen. However, it has to be noted that the unexpected high corrosion rate of material F containing all alloying elements distorts the picture. A direct comparison of the tested materials reveals a positive effect of Cr additions on the corrosion behavior. With the reference material containing 0.5 % Cr a reduction of the corrosion rate of 0.3 mm/y (-16 %) compared to the unalloyed steel was reached. Same effect was determined for the material with addition of 0.25 % Cu and 0.04 % V. Further increase of the V content to 0.08 % V resulted in an additional improvement of the CO₂ corrosion resistance with a reduction of the corrosion rate of about 30 % in total. These results confirm the positive effect reported for the addition of V in the literature [2, 10, 11]. Additions of 0.3 % Cr, 0.25 % Ni and 0.08 % V (material E) affected a similar decrease of the corrosion rate than addition of Cu and V showing that Cr and Ni yield no better effect compared to Cu. The increase of the corrosion rate determined for the higher alloyed material F show that apparently the combination of alloying elements could play a significant role regarding the CO₂ corrosion behavior. Thus, no real conclusion could be drawn for the effect of Mo.

An increase of the test temperature from 40 °C to 80 °C resulted in a decrease of the average corrosion rates as the formation of protective iron carbonate scales is facilitated under these conditions. The investigation of the samples revealed localized attack for the unalloyed steel as well as for the Cu containing materials C and D. Contradictory results regarding the effect of Cu can be found in the literature. While some authors reported a favorable effect of Cu [10, 11], others observed an increase of the susceptibility to localized corrosion [4, 7]. Material containing ≥ 0.3 % Cr showed a good resistance of the base metal to localized corrosion. However, preferential corrosion attack of the base material or at the transition of base metal to HAZ and weld were observed for almost all

materials. In addition, specimens revealed an improved corrosion resistance of the weld seam itself compared to the base material. Determined local differences of the corrosion rate indicate that the microstructure of weld metal, HAZ and base metal has a stronger influence on the corrosion attack than the effective addition of Cr or V. Against the background that the highly alloyed material F showed no localized attack at all it can be concluded that the addition of Cr and Mo has the highest effect for prevention of localized corrosion under the tested conditions.

CONCLUSIONS

Six alloying concepts with linepipe steel chemical compositions were defined and tested by means of laboratory melts with regard to an increase of the corrosion resistance in wet CO₂. The verification of suitable alloys was done by determination of the corrosion rate and the susceptibility to localized corrosion in the base metal and weld seam by rotating cage experiments in CO₂ containing 0.1 % sodium chloride solution.

With regard to uniform corrosion a favorable effect with a reduction of the corrosion rate of up to 30 % was yielded with the addition of Cr, Ni and V and with Cu and V while for the addition of Mo no clear conclusion can be drawn. By addition of beneficial elements such as Cr, Cu and Ni the combination of those elements appears to be relevant for the effect on the corrosion resistance.

Under conditions where localized corrosion dominates, best corrosion behavior was obtained for the higher alloyed materials containing at least 0.3 Cr which showed no localized corrosion of the base metal. With regard to the susceptibility of the HAZ the best corrosion resistance was achieved with the material containing all alloying elements. The addition of Cr and Mo seems to have the highest effect for prevention of localized corrosion under the tested conditions.

As alternative to 0.5 % Cr-steels the use of Cu, Ni and V containing alloys could be considered for conditions where uniform corrosion is expected. At increased operational temperatures a higher alloyed steel with Mo, Ni, Cu and V is the best alternative showing a low corrosion rate combined with a good resistance to localized corrosion of the base material and the HAZ.

REFERENCES

- [1] Schmitt, G.; Hörstemeier, M.: Fundamental Aspects of CO₂ Metal Loss Corrosion - Part II: Influence of Different Parameters on CO₂ Corrosion Mechanisms. CORROSION'2006, NACE International, Houston, TX, USA, 2006, paper no. 112
- [2] Dugstad, A.: Fundamental Aspects of CO₂ Metal Loss Corrosion - Part I: Mechanism. CORROSION'2006, NACE International, Houston, TX, USA, 2006, paper no. 111
- [3] Kermani, M.B.; Marshad, A.: Carbon Dioxide Corrosion in Oil and Gas Production - A Compendium. Corrosion, Vol.59, 2003, pp. 659-683
- [4] Kimura, M; Yoshiyuki, S.; Nakano, Y.: Effects of alloying elements on corrosion resistance of high strength line pipe steel in wet CO₂ environment. CORROSION'94, NACE International, Houston, TX, USA, 1994, paper no. 18
- [5] Bosch, C; Jansen, J.-P.; Poepperling, R. K.: Influence of Chromium Contents of 0.5 % to 1.0 % on the Corrosion Behaviour of Low Alloy Steel for Large-Diameter Pipes in CO₂ Containing Aqueous Media. CORROSION'03, NACE International, Houston, TX, 2003, paper no. 118

- [6] Dugstad, A.; Hemmer, H; Seiersten, M.: Effect of steel microstructure on corrosion rate and protective iron carbonate film formation. *Corrosion*, Vol.57, 2001, pp. 369-378
- [7] Dugstad, A.; Lunde, L.; Videm, K.: Influence of Alloying Elements upon the CO₂ Corrosion Rate of Low Alloyed Carbon Steels”, CORROSION’91, NACE International, Houston, TX, 1991, paper no. 473
- [8] Ueda, M.; Ikeda, A.: Effect of Microstructure and Cr Content in Steel on CO₂ Corrosion. CORROSION’96, NACE International, Houston, TX, 1996, paper no. 13
- [9] Nose, K.; Asahi, H.; Nice, P. I.; Martin, J.: Corrosion Properties of 3 % Cr Steels in Oil and Gas Environments. CORROSION’01, NACE International, Houston, TX, 2001, paper no. 82
- [10] Kermani, M. B.; Gonzales, J. C.; Linne, C.; Dougan, M.; Cochrane R.: Development of Low Carbon Cr-Mo Steels with Exceptional Corrosion Resistance for Oil-field Applications. CORROSION’01, NACE International, Houston, TX, 2001, paper no. 65
- [11] Kermani, M. B.; Gonzales, J. C.; Turconi, G. L.; Edmonds, D.; Dicken, G.; Scopio, L.: Development of Superior Corrosion Resistance 3% Cr Steels for Downhole Applications. CORROSION’03, NACE International, Houston, TX, 2003, paper no. 116
- [12] Muraki, T.; Nose, K.; Asahi, H.: Development of 3% Chromium Linepipe Steel. CORROSION’03, NACE International, Houston, TX, 2003, paper no. 117
- [13] Kermani, M. B.; Gonzales, J. C.; Turconi, G. L.; Perez, T; Morales, C.: Materials Optimisation in Hydrocarbon Production. CORROSION’05, NACE International, Houston, TX, 2005, paper no. 111
- [14] Edmonds, D.V.; Cochrane, R.C.:The Effect of Alloying on the Resistance of CarbonSteel for Oilfield Applications to CO₂ Corrosion. In: *Materials Research*, Vol. 8, No. 4, 2005, pp. 377-385
- [15] Lopez, D. A.; Perez, T.; Simison, S. N.: The influence of microstructure and chemical composition of carbon and low alloy steels in CO₂ corrosion. A state-of-the-art appraisal. In: *Materials & Design*, 2003, 24(8), pp. 561-575
- [16] Seiersten, M.; Dugstad, A.; Dougan, M.; Cochrane, R.: Flow Loop Testing of Microalloyed Low Carbon Cr-Mo Steels. Eurocorr’2001, Lake Garda, Italy, 2001
- [17] Al-hassan, S.; Mishra, B.; Olson, D.L.; Salama, M.M.: Effect of Microstructure on Corroding of Steels in Aqueous Solutions Containing Carbon Dioxide. *Corrosion*, Vol. 54, 1998, pp. 480-491